

Oxidative Synthesis of Bis(μ -hydroxo) Chromium(III) Dimers with Aromatic Amine Ligands. Structure, Physical Properties, and Base Hydrolysis Kinetics of the Bis(μ -hydroxo)bis{[tris(2-pyridylmethyl)amine]chromium(III)} Ion

Boyd G. Gafford and Robert A. Holwerda*

Received July 6, 1988

The purple bis(μ -hydroxo)bis{[tris(2-pyridylmethyl)amine]chromium(III)} ion and related bpy and phen diols have been prepared in excellent yields through the aerobic oxidation of chromium(II) in the presence of the aromatic amine ligands. Physical properties of [(tmpa)Cr(OH)₂Cr(tmpa)](ClO₄)₄·4H₂O include absorption peaks at 540 nm (ϵ 131 M⁻¹ cm⁻¹), 385 (113), and 261 (7850), an effective magnetic moment (295.15 K) of 3.57 μ_B , and hydroxo bridge ionization constants of $pK_{a1} = 7.50$ and $pK_{a2} = 12.4$ (25 °C, $I = 0.1$ M). Brown-green [(tmpa)CrO(OH)Cr(tmpa)](ClO₄)₃·H₂O was isolated pure in the solid state, but [(tmpa)-Cr(O)₂Cr(tmpa)]²⁺ undergoes facile base hydrolysis to [Cr(tmpa)(OH)₂]⁺. Crystals of [(tmpa)Cr(OH)₂Cr(tmpa)]Br₄·8H₂O are monoclinic with $a = 13.739$ Å, $b = 14.858$ Å, $c = 23.146$ Å, $\beta = 94.72^\circ$, $V = 4709$ Å³, space group C2/c, and a calculated density (for $Z = 4$) of 1.67 g cm⁻³. The structure was refined by full-matrix least-squares techniques to final agreement factors of $R_1 = 0.0658$ and $R_2 = 0.0649$. The Cr(1)-O(1) bond length and O-Cr-O and Cr-O-Cr angles characteristic of the Cr(OH)₂Cr core in the centrosymmetric dimer are 1.937 Å and 78.9 and 101.0°, respectively. The apical tmpa N atoms are trans with respect to the Cr₂O₂ core, in contrast to the molecular structure of [(tmpa)(SCN)CrOCr(NCS)(tmpa)]²⁺, derived from the reaction of thiocyanate ion with the diol, which has SCN⁻ ligands trans to both apical nitrogen atoms. The base hydrolysis of [(tmpa)Cr(O)₂Cr(tmpa)]²⁺ follows consecutive first-order kinetics in the range 0.10-1.00 M [OH⁻] ($I = 1.0$ M (NaOH/NaBr)), with both fast (89% of ΔA_{368}) and slow (11% of ΔA_{368}) components exhibiting parallel pathways of zero (k_0 and k_0' , respectively) and first order (k_{OH} and k_{OH}' , respectively) in hydroxide ion. Rate parameters are $k_0(25^\circ\text{C}) = 3.0 \times 10^{-4}$ s⁻¹ ($\Delta H^\ddagger = 19.9$ kcal mol⁻¹, $\Delta S^\ddagger = -8$ eu), $k_{OH}(25^\circ\text{C}) = 5.8 \times 10^{-4}$ M⁻¹ s⁻¹ ($\Delta H^\ddagger = 22.5$ kcal mol⁻¹, $\Delta S^\ddagger = +2$ eu), $k_0'(25^\circ\text{C}) = 4.7 \times 10^{-5}$ s⁻¹ ($\Delta H^\ddagger = 23$ kcal mol⁻¹, $\Delta S^\ddagger = -1$ eu), and $k_{OH}'(25^\circ\text{C}) = 2.7 \times 10^{-5}$ M⁻¹ s⁻¹ ($\Delta H^\ddagger = 28$ kcal mol⁻¹, $\Delta S^\ddagger = +14$ eu). The green base hydrolysis intermediate, thought to be [(tmpa)(OH)CrOCr(OH)(tmpa)]²⁺, was isolated by cation-exchange chromatography and shown to have spectroscopic characteristics (λ_{max} 580 nm (ϵ 85 M⁻¹ cm⁻¹), 364 (415)) consistent with the biphasic 368-nm kinetic results. The proposed mechanism features rate-limiting H₂O- and OH⁻-assisted Cr-O bond cleavages in [(tmpa)Cr(O)₂Cr(tmpa)]²⁺ and the binuclear intermediate, with the relative contributions of the hydroxide-dependent pathways being far smaller than is typical of chromium(III) base hydrolysis reactions.

Introduction

Considerable progress has been made recently in the understanding of magnetic¹ and spectroscopic² characteristics of bis(μ -hydroxo) chromium(III) dimers. The rates of ring-opening/ring-closing equilibria in acidic solutions of diols with aliphatic amine ligands have also been studied extensively.³ We are engaged in mechanistic studies of bridge-cleavage, substitution, and redox reactions of μ -oxo chromium(III) complexes and recently reported that an extensive class of [Cr(tmpa)L₂O]²⁺ cations could be prepared in excellent yield from the displacement of a hydroxo bridge in [(tmpa)Cr(OH)₂Cr(tmpa)]⁴⁺ by excess L in CH₃CN or aqueous solution⁴ (L = monodentate anionic ligand; tmpa = tris(2-pyridylmethyl)amine). A synthesis of the bis(μ -hydroxo)bis{[tris(2-pyridylmethyl)amine]chromium(III)} ion based on the aerobic oxidation of (tmpa)Cr^{II} is described in this paper, along with improved preparations of the analogous diols with 2,2'-bipyridine (bpy) and 1,10-phenanthroline (phen) ligands. Since [(bpy)₂Cr(OH)₂Cr(bpy)]⁴⁺ and [(phen)₂Cr(OH)₂Cr(phen)]⁴⁺ undergo single and double ionizations⁵ to give isolable μ -oxo hydroxo and bis(μ -oxo) species, respectively, the influence of oxo bridging on the thermodynamic and kinetic stabilities of these ionization products is also of interest. Considering that the bis(μ -oxo) forms of chromium(III) diols with aromatic amine ligands are known to decompose through bridge cleavage with

eventual loss of the N-donor groups,⁵ we have undertaken a kinetic study of [(tmpa)Cr(O)₂Cr(tmpa)]²⁺ base hydrolysis with the objective of determining whether a singly oxo-bridged intermediate is generated in the pathway leading to the mononuclear [Cr(tmpa)(OH)₂]⁺ product.

Experimental Section

Materials and Procedures. Reagent grade chemicals were used throughout. Gold Label chromium chunks (Aldrich), 98% 2-picoyl chloride hydrochloride (Aldrich), bis(2-pyridylmethyl)amine (Nepara), and 2,2'-bipyridine and 1,10-phenanthroline (G. F. Smith) were used as supplied. Solutions for spectroscopic and kinetic and ionization constant determinations were prepared from triply distilled water. Cation-exchange chromatography was performed on SP-Sephadex C-25-120 resin (Na⁺ form), and eluting solutions were prepared from doubly distilled water. Anaerobic preparations were carried out under chromous-scrubbed nitrogen, with use of Hamilton gastight syringes fitted with Teflon or stainless steel needles for solution transfers.

Stock solutions (150 mL) of Cr(ClO₄)₂ and CrBr₂ were prepared from the anaerobic reactions of excess Cr (8.00 g, 0.154 mol) with 0.300 mol of HClO₄ and HBr, respectively, in serum-capped bottles. These solutions were heated under continuous N₂ purge until H₂ evolution was no longer visible, at which time they were cooled to room temperature and standardized. Chromium chunks were treated with concentrated HClO₄ immediately prior to use in order to remove the surface oxide layer.

Tris(2-pyridylmethyl)amine was prepared through an adaptation of the literature method.⁶ 2-Picoyl chloride hydrochloride (48.4 g, 0.295 mol) was neutralized with 58.9 mL of 5.00 M NaOH (0.295 mol) and then combined with bis(2-pyridylmethyl)amine (58.7 g, 0.295 mol) while being stirred. Another 0.295 mol of NaOH was slowly added to the reaction mixture over the period of 1 h. The resulting brown solution was stirred at ambient temperature for 24 h and then neutralized with excess concentrated HClO₄, generating a tan precipitate of crude [H₃tmpa](ClO₄)₃ in 97% yield. Recrystallization and purification were accomplished in one step by preparing a solution 0.1 M in both [H₃tmpa](ClO₄)₃ and [Cr(H₂O)₆](ClO₄)₃ (to complex with impurities), adjusting the pH to 2.0 with HClO₄, and boiling for 15 min. The snow white crystals that formed upon cooling were washed with cold triply distilled water and air-dried. Anal. Calcd for [H₃tmpa](ClO₄)₃: C, 36.54; H,

- (1) (a) Hodgson, D. In *Magneto-Structural Correlations in Exchange Coupled Systems*; Willett, R. D., Ed.; Reidel: Dordrecht, The Netherlands, 1985; p 497. (b) Josephsen, J.; Pedersen, E. *Inorg. Chem.* **1977**, *16*, 2534.
- (2) (a) Riesen, H.; Reber, C.; Gudel, H. U.; Wiegardt, K. *Inorg. Chem.* **1987**, *26*, 2747. (b) Riesen, H.; Gudel, H. U. *Chem. Phys. Lett.* **1987**, *133*, 429.
- (3) (a) Springborg, J.; Toftlund, H. *Acta Chem. Scand., Ser. A* **1976**, *30*, 171. (b) Christensson, F.; Springborg, J.; Toftlund, H. *Acta Chem. Scand., Ser. A* **1980**, *34*, 317. (c) Christensson, F.; Springborg, J. *Acta Chem. Scand., Ser. A* **1982**, *36*, 21.
- (4) Gafford, B. G.; Holwerda, R. A.; Schugar, H. J.; Potenza, J. A. *Inorg. Chem.* **1988**, *27*, 1126.
- (5) Josephson, J.; Schaffer, E. *Acta Chem. Scand.* **1970**, *24*, 2929.

- (6) Anderegg, G.; Wenk, F. *Helv. Chim. Acta* **1971**, *51*, 224.

3.58; N, 9.47. Found: C, 36.37; H, 3.53; N, 9.27. UV (CH_3CN ; λ_{max} , nm (ϵ , $\text{M}^{-1} \text{cm}^{-1}$): 261 (14 400), 204 (9600).

Microanalyses were performed by Desert Analytics (Tucson, AZ). Chromium(II) and chromium(III) assays were carried out as previously described.⁷ Extinction coefficients are expressed per mole of Cr, except where otherwise noted.

Preparations of [(tmpa)Cr(OH)₂Cr(tmpa)](ClO₄)₄·4H₂O (I) and [(tmpa)Cr(OH)₂Cr(tmpa)]Br₄·8H₂O (II). [H_3tmpa](ClO₄)₃ (14.0 g, 0.0237 mol) was neutralized in 150 mL of vigorously stirred (10 min) 2.00 M NaOH. When the solution stood for an additional 10 min, the upper aqueous phase separated from the light tan tmpa oil, which was quantitatively collected with a syringe and injected into 150 mL of 95% ethanol. Aqueous Cr(ClO₄)₂ (0.0237 mol) was injected into this pale yellow ethanolic solution after purging with N₂ for 30 min, giving dark brown Cr(tmpa)(ClO₄)₂. The reaction mixture was then opened to the air and stirred vigorously, bringing about the rapid deposition of a fine purple powder, which was separated from a small amount of red byproduct by filtration. The slightly soluble product was recrystallized by dissolving in 900 mL of boiling 1.0 mM HClO₄, followed by adding LiClO₄ (3.0 g) and slowly cooling to room temperature. The resultant large maroon crystals of [(tmpa)Cr(OH)₂Cr(tmpa)](ClO₄)₄·4H₂O were washed with triply distilled water and air-dried; yield 13.43 g, 95%. Anal. Calcd for [(tmpa)Cr(OH)₂Cr(tmpa)](ClO₄)₄·4H₂O: Cr, 8.75; C, 36.38; H, 3.90; N, 9.43. Found: Cr, 8.73; C, 36.54; H, 3.77; N, 9.27. UV-vis (H_2O ; λ_{max} , nm (ϵ , $\text{M}^{-1} \text{cm}^{-1}$): 540 (131), 385 (113), 261 (7850). IR (KBr pellet; cm^{-1}): 3400 s, 3000 s, 1600 s, 1480 m, 1440 s, 1300 m, 1155 m, 1105 s, 1100 s, 1080 s, 1050 s, 1020 s, 940 w, 890 w, 770 s, 720 w, 650 s.

[(tmpa)Cr(OH)₂Cr(tmpa)]Br₄·8H₂O was prepared as described above for the perchlorate salt of the diol, with 15.0 g (0.0253 mol) of [H_3tmpa](ClO₄)₃, 0.0253 mol of aqueous CrBr₂, a 1.0 mM HBr (300 mL) recrystallization medium, and 20.0 g of NaBr added to the hot recrystallization solution before cooling. The crystalline purple product was washed with triply distilled water and air-dried; yield 13.8 g, 92%. Anal. Calcd for [(tmpa)Cr(OH)₂Cr(tmpa)]Br₄·8H₂O: Cr, 8.79. Found: Cr, 8.74. UV-vis (H_2O): identical with that for I. IR (KBr pellet; cm^{-1}): 3400 s, 3000 s, 1600 s, 1480 m, 1440 s, 1300 m, 1155 m, 1105 s, 1080 s, 1050 s, 1030 s, 940 w, 890 w, 770 s, 720 w, 650 s.

Preparation of [(tmpa)Cr(O)(OH)Cr(tmpa)](ClO₄)₃·H₂O (III). After I (1.00 g) was dissolved in 400 mL of water, the pH was adjusted to 10.0 by slow addition of 0.1 M NaOH. Solid LiClO₄ was then added until precipitation of the brown-green product commenced. The stirred solution was then cooled to 5 °C and digested for 30 min, at which time an 87% yield (0.76 g) of the crystalline product was isolated by filtration, washed quickly with cold distilled water, and air-dried. Anal. Calcd for [(tmpa)Cr(O)(OH)Cr(tmpa)](ClO₄)₃·H₂O: Cr, 10.06; C, 41.81; H, 3.80; N, 10.84. Found: Cr, 10.10; C, 41.65; H, 3.61; N, 10.68. UV-vis (H_2O ; λ_{max} , nm (ϵ , $\text{M}^{-1} \text{cm}^{-1}$): 370 (900), 258 (8900). IR (KBr pellet; cm^{-1}): 3400 s, 1600 s, 1480 m, 1440 s, 1300 m, 1155 m, 1105 s, 1100 s, 1080 s, 1050 s, 1030 s, 940 w, 890 w, 770 s, 720 w, 650 s. Several attempts to isolate [(tmpa)Cr(O)₂Cr(tmpa)](ClO₄)₂ as a pure solid from solutions at pH 12 or above failed because of the facile base hydrolysis reaction of the dioxo dimer.

Preparation of [Cr(tmpa)(SCN)₂](ClO₄) (IV). Method A. A solution of I (1.00 g, 0.841 mmol) mixed with 1.68 mmol of NaOH in 200 mL of water was boiled for 10 min, resulting in the quantitative formation of blue [Cr(tmpa)(OH)₂]⁺. After the dihydroxo monomer was converted to red [Cr(tmpa)(OH)₂]³⁺ through the addition of 1.75 mL of 11.45 M HClO₄, NaSCN (5.46 g, 67.4 mmol) was added and the solution was boiled with stirring for 60 min. The brick red precipitate that formed upon cooling to room temperature was washed with triply distilled water and air-dried; yield 0.890 g, 95%. Anal. Calcd for [(tmpa)Cr(NCS)₂](ClO₄): Cr, 9.32. Found: Cr, 9.25. UV-vis (CH_3CN ; λ_{max} , nm (ϵ , $\text{M}^{-1} \text{cm}^{-1}$): 515 (210), 348 (8700), 324 sh (6100), 261 (12 300). IR (KBr pellet; cm^{-1}): 3400 m, 2020 s, 1600 m, 1480 w, 1440 m, 1280 w, 1300 w, 1100 s, 1030 m, 900 w, 770 m, 740 w, 650 w.

Method B. I (1.00 g, 0.841 mmol) was allowed to react with NaSCN (5.46 g, 67.4 mmol) at pH 1.5 (HClO₄) for 2 h in 500 mL of boiling water, with an accompanying color change from purple to bright red and reduction of the solution volume to 300 mL. When the solution was cooled to room temperature, a 75% yield (0.700 g) of the product crystallized and was recovered as in method A. Anal. Calcd for [(tmpa)Cr(NCS)₂](ClO₄): Cr, 9.32; C, 43.05; H, 3.25; N, 15.06. Found: Cr, 9.27; C, 43.08; H, 3.43; N, 15.49. UV-vis (CH_3CN) and IR (KBr pellet): identical with those for the product from method A.

Preparation of [(bpy)₂Cr(OH)₂Cr(bpy)₂](ClO₄)₄·2H₂O. 2,2'-Bipyridine (10.0 g, 0.064 mol) was dissolved in 100 mL of 95% ethanol,

and the solution was purged with N₂ for 30 min. A dark purple precipitate and solution were observed upon the anaerobic injection of aqueous Cr(ClO₄)₂ (0.032 mol). When this mixture was stirred in the presence of oxygen, the purple intermediate slowly converted to a reddish tan precipitate of [(bpy)₂Cr(OH)₂Cr(bpy)₂](ClO₄)₄·2H₂O. The product was recrystallized as above (diol I), washed with triply distilled water, and air-dried; yield 14.5 g, 72%. Anal. Calcd for [(bpy)₂Cr(OH)₂Cr(bpy)₂](ClO₄)₄·2H₂O: Cr, 8.69; C, 40.15; H, 3.03; N, 9.36. Found: Cr, 8.31; C, 40.39; H, 2.87; N, 9.41. UV-vis (5.0 mM HClO₄(aq); λ_{max} , nm (ϵ , $\text{M}^{-1} \text{cm}^{-1}$): 310 (20 800), 392 (344), 416 sh (228), 428 sh (80), 533 (55).

Preparation of [(phen)₂Cr(OH)₂Cr(phen)₂](ClO₄)₄·3H₂O. Cr(ClO₄)₂ (0.0253 mol) was injected into an anaerobic solution of 1,10-phenanthroline (10.0 g, 0.0505 mol) dissolved in 100 mL of 95% ethanol, giving a dark brown reaction mixture that deposited a tan precipitate of [(phen)₂Cr(OH)₂Cr(phen)₂](ClO₄)₄·3H₂O upon subsequent aerobic stirring. Product workup was identical with that employed for the bpy diol; yield 12.2 g, 74%. Anal. Calcd for [(phen)₂Cr(OH)₂Cr(phen)₂](ClO₄)₄·3H₂O: C, 43.99; H, 2.92; N, 8.55. Found: C, 44.18; H, 2.68; N, 8.55. UV-vis (CH_3CN ; λ_{max} , nm (ϵ , $\text{M}^{-1} \text{cm}^{-1}$): 226 (58 000), 276 (40 400), 353 (1740), 538 (55).

Ionization Constant Determinations. A 367-nm spectrophotometric titration⁸ was performed to determine the first (K_{a1}) and second (K_{a2}) ionization constants of the [(tmpa)Cr(OH)₂Cr(tmpa)]⁴⁺ ion. *N,N*-Bis-(2-hydroxyethyl)-2-aminoethanesulfonic acid (BES) and carbonate buffers (10 mM) containing 0.1 M NaNO₃ were used in the pH 6.4–10.6 range, while HNO₃ or NaOH solutions adjusted to a constant ionic strength of 0.1 M with NaNO₃ extended the pH interval down to 1 and up to 13. A 1.00 mM solution of I in 0.1 M NaNO₃ was mixed with the identical volume of the pH-controlling solution, both thermostated at 25.0 °C, and the absorbance was quickly determined in a 1-cm quartz cell. One determination was carried out in 3.2 M NaOH in order to better define the limiting absorbance at high pH. Hydrogen ion concentrations were derived from pH readings (Brinkmann 104 pH meter) as previously described.⁹ The ionization constants K_{a1} and K_{a2} and extinction coefficients of un-ionized (ϵ_0) and singly (ϵ_1) and doubly ionized (ϵ_2) diol species were extracted from a nonlinear least-squares fit (method of steepest descent) of the A_{367} vs $[\text{H}^+]$ data to relationships 1, where C_0 represents the total dimer concentration ($[\text{Cr}(\text{OH})_2\text{Cr}^{4+}] + [\text{Cr}(\text{OH})(\text{O})\text{Cr}^{3+}] + [\text{Cr}(\text{O})_2\text{Cr}^{2+}]$).

$$A_{367} = \epsilon_0[\text{Cr}(\text{OH})_2\text{Cr}^{4+}] + \epsilon_1[\text{Cr}(\text{OH})(\text{O})\text{Cr}^{3+}] + \epsilon_2[\text{Cr}(\text{O})_2\text{Cr}^{2+}]$$

$$[\text{Cr}(\text{OH})_2\text{Cr}^{4+}] = C_0 / (1 + K_{a1}/[\text{H}^+] + K_{a1}K_{a2}/[\text{H}^+]^2)$$

$$[\text{Cr}(\text{OH})(\text{O})\text{Cr}^{3+}] = C_0 / (1 + [\text{H}^+]/K_{a1} + K_{a2}/[\text{H}^+])$$

$$[\text{Cr}(\text{O})_2\text{Cr}^{2+}] = C_0 / (1 + [\text{H}^+]/K_{a2} + [\text{H}^+]^2/K_{a1}K_{a2}) \quad (1)$$

Kinetic Measurements. The kinetics of [(tmpa)Cr(O)₂Cr(tmpa)]²⁺ base hydrolysis was monitored at 368 nm in 1-cm cells thermostated at six temperatures in the range 20.6–45.0 °C. The hydroxide ion concentration dependence of the rate was investigated in solutions containing 0.1–1.0 M NaOH and sufficient NaBr to maintain a constant ionic strength of 1.0 M; NaBr was shown to have no effect on the rate or product distribution of the base hydrolysis reaction and was used in place of NaClO₄ because of the insolubility of the tmpa diol species in perchlorate media. The chromium reactant was generated in situ by injecting sufficient [(tmpa)Cr(OH)₂Cr(tmpa)]Br₄ to give an initial dioxo dimer concentration of 0.375 mM. Pseudo-first-order rate constants for the fast (k_{fast}) and slow (k_{slow}) components of biphasic $\ln(A_t - A_\infty)$ vs time traces were extracted from a consecutive first-order analysis.¹⁰ Least-squares fits of the kinetic data to this consecutive first-order scheme were found to be excellent over the entire hydroxide concentration and temperature ranges examined. Reported rate parameters are the mean values of at least three determinations.

Instrumentation. Ultraviolet-visible and infrared spectra were acquired on Shimadzu UV-260 and Beckman Acculab 8 spectrophotometers, respectively, and kinetic measurements were carried out on a Perkin-Elmer Lambda 5 instrument. Magnetic susceptibility determinations were performed at ambient temperature on a Johnson-Matthey magnetic susceptibility balance, calibrated against Hg[Co(SCN)₄]. Reported magnetic moments are uncorrected for ligand and counterion diamagnetism.

(8) Holwerda, R. A.; Clemmer, J. D. *Inorg. Chem.* **1982**, *21*, 2103.

(9) Baek, H. B.; Holwerda, R. A. *Inorg. Chem.* **1983**, *22*, 3452.

(10) Espenson, J. H. *Chemical Kinetics and Reaction Mechanisms*; McGraw-Hill: New York, 1981.

Table I. Crystallographic Data for $[(\text{tmpa})\text{Cr}(\text{OH})_2\text{Cr}(\text{tmpa})]\text{Br}_4 \cdot 8\text{H}_2\text{O}^a$

formula	$\text{C}_{36}\text{H}_{54}\text{N}_8\text{O}_{10}\text{Cr}_2\text{Br}_4$	molecules/unit cell	4
fw	1182.49	$\rho(\text{calcd})$, g cm^{-3}	1.67
space group	monoclinic, $C2/c$	temp, $^\circ\text{C}$	22
cell constants		μ , cm^{-1}	37.8
a , Å	13.739 (5)	radiation	Mo K α ; $\lambda =$
b , Å	14.858 (5)		0.710 73 Å
c , Å	23.146 (9)	R_1	0.0658
β , deg	94.72 (3)	R_2	0.0649
cell vol, Å^3	4709 (3)		

^aUncertainties in the last significant digit are shown in parentheses.

Table II. Atomic Coordinates ($\times 10^4$) and Equivalent Isotropic Displacement Parameters ($\text{Å}^2 \times 10^3$) for $[(\text{tmpa})\text{Cr}(\text{OH})_2\text{Cr}(\text{tmpa})]\text{Br}_4 \cdot 8\text{H}_2\text{O}^a$

atom	x	y	z	$U(\text{eq})$
Cr(1)	4976 (2)	5756 (1)	4568 (1)	13 (1)
O(1)	4190 (6)	4750 (5)	4785 (3)	36 (3)
N(1)	5866 (8)	6800 (7)	4390 (5)	39 (4)
C(11A)	6775 (10)	6404 (10)	4171 (6)	47 (6)
C(12A)	6507 (11)	5602 (9)	3795 (7)	41 (6)
C(13A)	7023 (11)	5383 (12)	3336 (7)	58 (7)
C(14A)	6718 (14)	4609 (13)	3022 (8)	75 (9)
C(15A)	5930 (14)	4135 (11)	3168 (7)	66 (8)
C(16A)	5446 (10)	4428 (10)	3625 (6)	40 (5)
N(1A)	5722 (8)	5152 (7)	3942 (4)	31 (4)
C(11B)	6079 (10)	7273 (9)	4953 (6)	45 (6)
C(12B)	5143 (11)	7362 (10)	5217 (6)	37 (6)
C(13B)	4949 (12)	8058 (11)	5579 (7)	55 (7)
C(14B)	4089 (16)	8089 (10)	5833 (8)	70 (8)
C(15B)	3384 (12)	7441 (12)	5684 (7)	60 (7)
C(16B)	3579 (11)	6743 (10)	5325 (6)	44 (6)
N(1B)	4463 (9)	6715 (7)	5095 (5)	39 (4)
C(11C)	5321 (10)	7421 (9)	3952 (6)	47 (6)
C(12C)	4454 (10)	7016 (8)	3644 (6)	33 (5)
C(13C)	3984 (13)	7389 (10)	3159 (7)	60 (7)
C(14C)	3148 (13)	7009 (11)	2912 (6)	59 (7)
C(15C)	2790 (11)	6234 (11)	3146 (7)	55 (7)
C(16C)	3283 (9)	5866 (9)	3612 (6)	38 (5)
N(1C)	4103 (8)	6248 (7)	3877 (5)	39 (4)
Br(1)	1899 (1)	8198 (1)	1586 (1)	74 (1)
Br(2)	1809 (1)	4742 (1)	4698 (1)	86 (1)
O(1W)	8741 (13)	4144 (11)	4273 (6)	186 (10)
O(2W)	4274 (10)	11553 (11)	2885 (6)	164 (9)
O(3W)	5500 (13)	10078 (10)	6694 (10)	233 (13)
O(4W)	8772 (12)	5834 (12)	7010 (9)	244 (14)

^aEquivalent isotropic U is defined as one-third of the trace of the orthogonalized U_{ij} tensor. Uncertainties in the last significant digit are shown in parentheses.

X-ray Diffraction Studies. The structure of $[(\text{tmpa})\text{Cr}(\text{OH})_2\text{Cr}(\text{tmpa})]\text{Br}_4 \cdot 8\text{H}_2\text{O}$ was solved by direct methods on a Nicolet R3m/V diffractometer, utilizing 2428 unique reflections ($I > 3\sigma(I)$). In full-matrix least-squares refinements (SHELXTL PLUS), all non-hydrogen atoms were refined independently with anisotropic thermal parameters. The largest peak in a final difference map was 0.69 Å^{-3} . Details of the crystal data, experimental conditions, and a summary of refinement details are given in Table I; Table II presents the atomic coordinates and isotropic displacement parameters.

Results and Discussion

The syntheses of $[(\text{tmpa})\text{Cr}(\text{OH})_2\text{Cr}(\text{tmpa})]\text{ClO}_4 \cdot 4\text{H}_2\text{O}$ and the corresponding bromide salt in high yields were easily accomplished through the aerobic oxidation of $(\text{tmpa})\text{Cr}^{\text{II}}$. Analogous preparations of $[(\text{bpy})_2\text{Cr}(\text{OH})_2\text{Cr}(\text{bpy})_2](\text{ClO}_4)_4 \cdot 2\text{H}_2\text{O}$ and $[(\text{phen})_2\text{Cr}(\text{OH})_2\text{Cr}(\text{phen})_2](\text{ClO}_4)_4 \cdot 3\text{H}_2\text{O}$ reproduced the compounds reported previously⁵ from the direct reactions of chromium(III) with the aromatic amine ligands in refluxing HClO_4 over extended time periods. We also note that Hodgson and co-workers recently reported the synthesis of $[(\text{tmpa})\text{Cr}(\text{OH})_2\text{Cr}(\text{tmpa})](\text{ClO}_4)_4 \cdot 4\text{H}_2\text{O}$ in 30% yield from the gradual addition of LiOH to a refluxing mixture of $[\text{H}_3\text{tmpa}](\text{ClO}_4)_3$ with chromium(III) nitrate, requiring a total reaction time of 5 h.¹¹

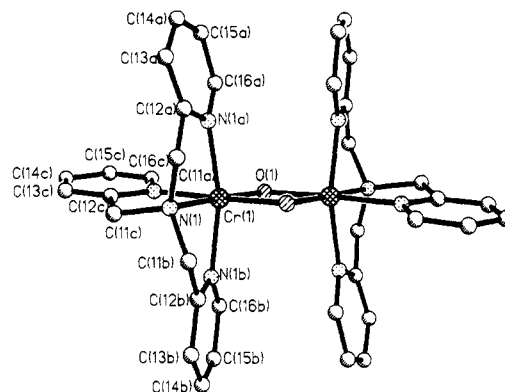


Figure 1. View of the $[(\text{tmpa})\text{Cr}(\text{OH})_2\text{Cr}(\text{tmpa})]^{4+}$ cation (H atoms excluded) in II. Selected interatomic distances (Å) and angles (deg) are as follows: $\text{Cr}(1)-\text{O}(1) = 1.937(8)$, $\text{Cr}(1)-\text{N}(1) = 2.041(11)$, $\text{Cr}(1)-\text{N}(1a) = 2.052(11)$, $\text{Cr}(1)-\text{N}(1b) = 2.041(12)$, $\text{Cr}(1)-\text{N}(1c) = 2.052(11)$, $\text{N}(1)-\text{Cr}(1)-\text{O}(1) = 176.0(4)$, $\text{N}(1a)-\text{Cr}(1)-\text{O}(1) = 99.7(4)$, $\text{N}(1a)-\text{Cr}(1)-\text{N}(1) = 81.2(5)$, $\text{N}(1b)-\text{Cr}(1)-\text{O}(1) = 99.0(4)$, $\text{N}(1b)-\text{Cr}(1)-\text{N}(1) = 80.3(5)$, $\text{N}(1b)-\text{Cr}(1)-\text{N}(1a) = 161.2(4)$, $\text{N}(1c)-\text{Cr}(1)-\text{O}(1) = 100.1(4)$, $\text{N}(1c)-\text{Cr}(1)-\text{N}(1) = 83.9(4)$, $\text{N}(1c)-\text{Cr}(1)-\text{N}(1a) = 84.2(4)$, $\text{N}(1c)-\text{Cr}(1)-\text{N}(1b) = 90.5(4)$. Uncertainties in the last significant digit are shown in parentheses.

Like the bipyridine and phenanthroline diols, $[(\text{tmpa})\text{Cr}(\text{OH})_2\text{Cr}(\text{tmpa})]^{4+}$ ionizes to give oxo hydroxo and dioxo dimers, but only the former could be isolated pure in the solid state. The generality of oxidative chromium(III) diol synthesis in the presence of aromatic amine ligands is further indicated by the preparation of $[(\text{dmpa})\text{Cr}(\text{SO}_4)(\text{OH})_2\text{Cr}(\text{dmpa})](\text{S}_2\text{O}_8) \cdot 3\text{H}_2\text{O}$ ¹² ($\text{dmpa} = \text{bis}(2\text{-pyridylmethyl})\text{amine}$) from the aerobic oxidation of a CrSO_4 - dmpa mixture.

X-ray diffraction analysis of $[(\text{tmpa})\text{Cr}(\text{OH})_2\text{Cr}(\text{tmpa})]\text{Br}_4 \cdot 8\text{H}_2\text{O}$ (Figure 1) revealed a centrosymmetric dimer possessing a highly distorted octahedral N_4O_2 coordination sphere about Cr. The $\text{Cr}-\text{O}-\text{Cr}$ (101.0°) and $\text{O}-\text{Cr}-\text{O}$ (78.9°) angles defined by the $\text{Cr}(\text{OH})_2\text{Cr}$ core closely resemble those reported for $[(\text{H}_2\text{O})_4\text{Cr}(\text{OH})_2\text{Cr}(\text{H}_2\text{O})_4]^{4+}$ (101.8 and 78.2° , respectively)¹³ and an extensive family of $\text{N}_4\text{Cr}(\text{OH})_2\text{CrN}_4$ dimers.¹⁴ While the present work was in progress, Hodgson and co-workers reported the structure of $[(\text{tmpa})\text{Cr}(\text{OH})_2\text{Cr}(\text{tmpa})](\text{ClO}_4)_4 \cdot 4\text{H}_2\text{O}$, noting that two possible isomers are distinguished by having the two bridgehead N atoms either cis or trans relative to the Cr_2O_2 core.¹¹ Our investigation of $[(\text{tmpa})\text{Cr}(\text{OH})_2\text{Cr}(\text{tmpa})]\text{Br}_4 \cdot 8\text{H}_2\text{O}$ confirms their prediction (on steric grounds) and finding that the trans, centrosymmetric form should be preferred over the cis isomer.¹¹ Vital structural parameters characteristic of the perchlorate salt,¹¹ including both bond lengths and angles from Cr to ligated N and O atoms, agree well with those reported here.

As compared with that in the linear $[(\text{tmpa})(\text{SCN})\text{CrO}(\text{NCS})(\text{tmpa})]^{2+}$ dimer,⁴ the $\text{Cr}(1)-\text{O}(1)$ bond length in the diol is considerably longer (1.937 vs 1.800 Å) while the Cr -pyridyl N distances are somewhat shorter (average of 2.048 vs 2.090 Å). Overall, the conformations of the tmpa pyridine rings in the oxo- and dihydroxo-bridged dimers are quite similar. An important structural distinction should be noted, however, with implications for the mechanism of hydroxo bridge displacement by SCN^- in the conversion of $[(\text{tmpa})\text{Cr}(\text{OH})_2\text{Cr}(\text{tmpa})]^{4+}$ to $[(\text{tmpa})(\text{SCN})\text{CrO}(\text{NCS})(\text{tmpa})]^{2+}$, which occurs readily in both acetonitrile and aqueous solutions.⁴ Whereas the apical tmpa nitrogen atoms of the diol are trans to hydroxo bridge O(1) and O(2) atoms, the apical nitrogens of the oxo-bridged dimer are both trans to thiocyanate ligands. It is not obvious how the substitution of one OH^- bridge by two nonbridging nucleophiles induces the rearrangement of the two tetradentate tmpa ligands such that *neither* of the nitrogen atoms originally trans to oxygen retains that orientation in the $\text{Cr}-\text{O}-\text{Cr}$ product. The mechanism of anion

(12) Larsen, S.; Michelson, K.; Pedersen, E. *Acta Chem. Scand., Ser. A* **1986**, *40*, 63.

(13) Spiccia, L.; Stoeckli-Evans, W.; Marty, W.; Giovanoli, R. *Inorg. Chem.* **1987**, *26*, 474.

(11) Hodgson, D. J.; Zietlow, M. H.; Pedersen, E.; Toftlund, H. *Inorg. Chim. Acta* **1988**, *149*, 111.

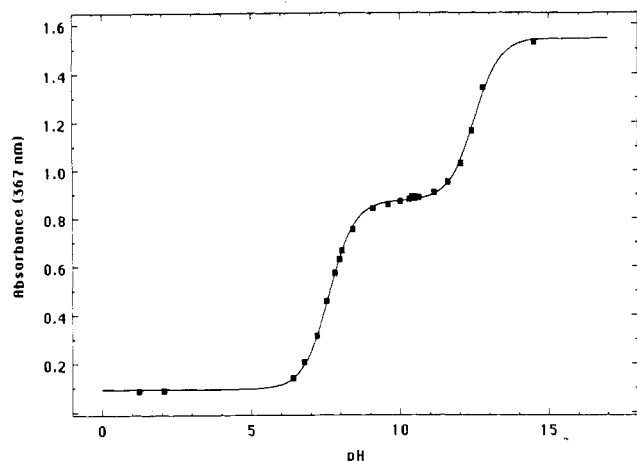


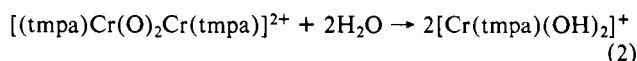
Figure 2. Spectrophotometric titration of $[(\text{tmpa})\text{Cr}(\text{OH})_2\text{Cr}(\text{tmpa})]^{4+}$ at 367 nm (25.0 °C, $I = 0.1$ M (NaNO_3), 1 cm path length, $C_0 = 0.5$ mM).

attack on $[(\text{tmpa})\text{Cr}(\text{OH})_2\text{Cr}(\text{tmpa})]^{4+}$, which necessarily requires either Cr–N or Cr–O bond migrations, is currently under investigation.¹⁴

Both spectroscopic and magnetic characteristics of $[(\text{tmpa})\text{Cr}(\text{OH})_2\text{Cr}(\text{tmpa})]^{4+}$ are consistent with expectations for a weakly antiferromagnetically coupled dimer. The magnetic susceptibility (295.15 K) of I was found to be $(9.10 \pm 0.10) \times 10^{-6}$ cgsu, equivalent to μ_{eff} value of $3.57 \pm 0.05 \mu_{\text{B}}$ per chromium atom; Hodgson and co-workers report¹¹ a singlet–triple energy gap ($-2J$) of 30.58 cm^{-1} . The diol UV–visible spectrum exhibits only three prominent features, including d–d bands at 18 500 ($=10Dq$) and 26 000 cm^{-1} ; the intense 38 300- cm^{-1} band is assigned to a tmpa ligand-centered π – π^* transition, by comparison with the spectrum of $[\text{H}_3\text{tmpa}](\text{ClO}_4)_3$. The electronic spectrum of $[(\text{tmpa})\text{Cr}(\text{OH})_2\text{Cr}(\text{tmpa})]^{4+}$ reported here is in reasonable agreement with that in the literature.¹¹ The magnetic susceptibility (295.15 K) of the oxo hydroxo dimer III is $(6.05 \pm 0.10) \times 10^{-6}$ cgsu, giving a μ_{eff} value of $2.72 \pm 0.05 \mu_{\text{B}}$ (or approximately two unpaired electrons) per chromium atom. Monomer IV exhibits a magnetic susceptibility (296.95 K) of $(11.0 \pm 0.10) \times 10^{-6}$ cgsu, corresponding to an effective magnetic moment ($3.82 \pm 0.05 \mu_{\text{B}}$) close to the spin-only value for three unpaired electrons per Cr atom ($3.87 \mu_{\text{B}}$).

Ionization constants (25.0 °C, $I = 0.1$ M) of the $[(\text{tmpa})\text{Cr}(\text{OH})_2\text{Cr}(\text{tmpa})]^{4+}$ ($\text{p}K_{\text{a}1} = 7.50 \pm 0.05$) and $[(\text{tmpa})\text{Cr}(\text{O})(\text{OH})\text{Cr}(\text{tmpa})]^{3+}$ ($\text{p}K_{\text{a}2} = 12.4 \pm 0.1$) ions, derived from a 367-nm spectrophotometric titration (Figure 2) of diol I, are quite similar to the literature values⁵ for the corresponding bpy ($\text{p}K_{\text{a}1} = 7.60$; $\text{p}K_{\text{a}2} = 11.9$) and phen ($\text{p}K_{\text{a}1} = 7.40$; $\text{p}K_{\text{a}2} = 11.8$) dimers. Nonlinear least-squares extinction coefficients (eq 1, expressed per mole of dimer) are $\epsilon_0 = 188 \pm 12$, $\epsilon_1 = 1750 \pm 10$, and $\epsilon_2 = 3090 \pm 20 \text{ M}^{-1} \text{ cm}^{-1}$. The last two values are in excellent agreement with the 367-nm extinction coefficients measured directly (per mole of dimer) for $[(\text{tmpa})\text{Cr}(\text{O})(\text{OH})\text{Cr}(\text{tmpa})]^{3+}$ ($1760 \text{ M}^{-1} \text{ cm}^{-1}$) and $[(\text{tmpa})\text{Cr}(\text{O})_2\text{Cr}(\text{tmpa})]^{2+}$ ($3060 \text{ M}^{-1} \text{ cm}^{-1}$) at pH 10.0 and 14.5, respectively. Although $[(\text{tmpa})\text{Cr}(\text{O})_2\text{Cr}(\text{tmpa})]^{2+}$ is considerably more susceptible to decomposition in basic solution than the bpy and phen dioxo dimers,⁵ the two-step ionization of $[(\text{tmpa})\text{Cr}(\text{OH})_2\text{Cr}(\text{tmpa})]^{4+}$ was shown to be quite reversible when the $\text{Cr}(\text{O})_2\text{Cr}$ complex was not allowed to stand at 25.0 °C for longer than 15 s.

The base hydrolysis reaction of $[(\text{tmpa})\text{Cr}(\text{O})_2\text{Cr}(\text{tmpa})]^{2+}$ proceeds according to the stoichiometry of eq 2 and gives no chromium byproducts detectable by cation-exchange chromatography. In support of this stoichiometry, it was demonstrated



that 2.00 ± 0.01 mol of OH^- is consumed per mole of un-ionized

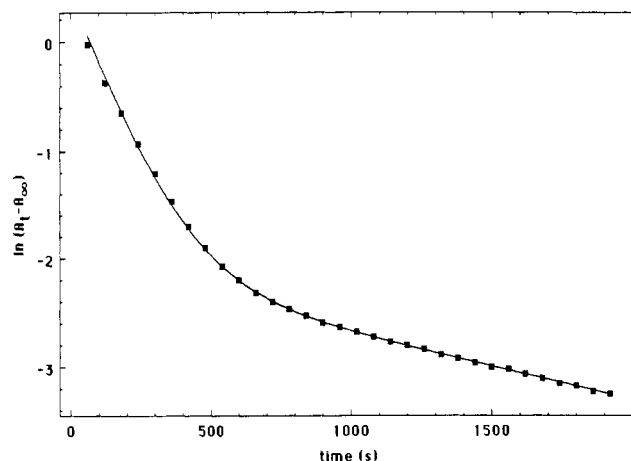


Figure 3. Typical $\ln(A_t - A_\infty)$ (368 nm) vs time plot for the biphasic hydrolysis reaction of $[(\text{tmpa})\text{Cr}(\text{O})_2\text{Cr}(\text{tmpa})]^{2+}$ (40.0 °C, $I = [\text{OH}^-] = 1.0$ M). The solid curve was drawn from the least-squares consecutive first-order rate parameters.

diol reactant consumed. I (0.841 mmol) was added to 200 mL of distilled water originally at pH 7.75, and the temperature was raised to the boiling point, giving a clear, deep purple solution. Upon the addition of 1.68 mmol of NaOH, the color changed immediately to dark green and transformed to dark blue after continued heating for 10 min. The pH of the cooled product solution was found to be 8.30, and a single blue band (complex V) was eluted from a SP-Sephadex C-25 cation-exchange column (0.1 M LiClO_4 eluent at pH 10.0).

Attempts to isolate the blue diol base hydrolysis product in crystalline form were unsuccessful with several counterions (ClO_4^- , $\text{S}_2\text{O}_6^{2-}$, SO_4^{2-}), owing to the very high solubility of V and its tendency to lose tmpa upon long standing in alkaline media, analogous to the behaviors of the bpy and phen diol systems.⁵ Taken together, stoichiometric, spectrophotometric, and derivative preparation results provide a convincing basis for attributing the formula $[\text{Cr}(\text{tmpa})(\text{OH})_2]^{+}$ to V, which exhibits d–d absorptions at 401 nm ($\epsilon 68 \text{ M}^{-1} \text{ cm}^{-1}$) and 578 (53). Upon acidification, V is reversibly protonated (in the pH 2–4 range) to a red complex (VI) ($\lambda_{\text{max}} 375 \text{ nm}$ ($\epsilon 71 \text{ M}^{-1} \text{ cm}^{-1}$), 501 (91)), which is thought to be $[\text{Cr}(\text{tmpa})(\text{H}_2\text{O})_2]^{3+}$. The relative positions of the lowest energy ($=10Dq$) spin-allowed bands of V, $[(\text{tmpa})\text{Cr}(\text{OH})_2\text{Cr}(\text{tmpa})]^{4+}$, and VI at 17 300, 18 500, and 20 000 cm^{-1} respectively are consistent with the spectrochemical series $\text{OH}^- < \text{bridging OH}^- < \text{H}_2\text{O}$. Like $[\text{Cr}(\text{tmpa})(\text{OH})_2]^{+}$, $[\text{Cr}(\text{tmpa})(\text{H}_2\text{O})_2]^{3+}$ is highly soluble and could not be precipitated in pure form; LiClO_4 crystallized before VI in perchlorate media. For this reason, VI was converted to $[\text{Cr}(\text{tmpa})(\text{NCS})_2](\text{ClO}_4)$ in the presence of excess thiocyanate to provide evidence for a monomeric precursor with two replaceable ligands derived from the solvent. The elemental analysis, magnetic susceptibility, and infrared and UV–visible spectra of complex IV indicate a simple Cr(III) monomer with a N_6 ligand field. It should also be noted that IV could be obtained from diol I upon extended heating in the presence of excess NaSCN, under conditions where the acid hydrolysis of I was shown to be negligible. The red species attributed to $[\text{Cr}(\text{tmpa})(\text{H}_2\text{O})_2]^{3+}$ did not give the characteristic spectrum of $[(\text{tmpa})\text{Cr}(\text{O})(\text{OH})\text{Cr}(\text{tmpa})]^{3+}$ when the pH was raised to 10, indicating the absence of $[(\text{tmpa})\text{Cr}(\text{OH})_2\text{Cr}(\text{tmpa})]^{4+}$ in re-acidified solutions of the diol base hydrolysis product.

Biphasic plots of $\ln(A_t - A_\infty)$ vs time observed in kinetic studies of reaction 2 ($[\text{OH}^-] = 0.1$ – 1.0 M) were successfully fit to the integrated rate expression for consecutive first-order reactions, as exemplified by Figure 3. Repetitive spectra (300–700 nm) recorded over the entire period of the base hydrolysis reaction demonstrated that absorbance decreases at the monitoring wavelength of 368 nm are typical of those observed throughout the entire wavelength interval. Rate measurements at pH < 12 demonstrated that the base hydrolysis reactivity of $[(\text{tmpa})\text{Cr}(\text{O})(\text{OH})\text{Cr}(\text{tmpa})]^{3+}$ is negligible¹⁵ as compared with that of

Table III. Rate Constants for Base Hydrolysis of the $[(\text{tmpa})\text{Cr}(\text{O})_2\text{Cr}(\text{tmpa})]^{2+}$ Ion^a

temp, °C	[OH ⁻], M	$10^3 k_{\text{fast}}$, s ⁻¹	$10^4 k_{\text{slow}}$, s ⁻¹
20.6	0.200	0.283	0.248
	0.500	0.401	0.274
	0.700	0.459	0.291
	1.00	0.574	0.315
26.1	0.200	0.547	0.435
	0.500	0.748	0.526
	0.700	0.924	0.606
	1.00	1.16	0.700
29.9	0.200	0.856	0.848
	0.500	1.24	1.06
	0.700	1.61	1.31
	1.00	2.00	1.39
35.0	0.200	1.23	1.10
	0.500	1.86	1.48
	0.700	2.60	1.83
	1.00	3.17	2.10
40.0	0.100	2.68	
	0.200	3.14	5.04
	0.300	3.87	
	0.400	4.06	
	0.500	4.80	5.94
	0.600	5.20	
45.0	0.700	5.46	5.82
	0.800	5.91	
	0.900	6.42	
	1.00	6.84	6.33
	0.200	4.21	4.48
0.500	6.34	6.76	
	0.700	8.23	7.66
1.00	9.99	8.80	

^a $I = 1.0$ M (NaOH/NaBr). Rate constants of the fast (k_{fast}) and slow (k_{slow}) phases of the consecutive first-order decomposition reaction were derived as described in the text. Uncertainties in k_{fast} and k_{slow} are estimated at $\pm 3\%$ and $\pm 6\%$, respectively.

Table IV. Rate Parameters for the Base Hydrolysis of $[(\text{tmpa})\text{Cr}(\text{O})_2\text{Cr}(\text{tmpa})]^{2+}$ ^a

temp, °C	$10^3 k_{\text{O}}$, s ⁻¹	$10^3 k_{\text{OH}}$, M ⁻¹ s ⁻¹	$10^4 k_{\text{O}}^{\text{s}}$, s ⁻¹	$10^4 k_{\text{OH}}^{\text{s}}$, M ⁻¹ s ⁻¹
20.6	0.214 (0.008)	0.359 (0.012)	0.232 (0.001)	0.0838 (0.0012)
26.1	0.381 (0.019)	0.773 (0.028)	0.366 (0.008)	0.335 (0.012)
29.9	0.554 (0.047)	1.45 (0.07)	0.725 (0.083)	0.711 (0.012)
35.0	0.715 (0.140)	2.50 (0.22)	0.860 (0.071)	1.28 (0.11)
40.0	2.33 (0.09)	4.56 (0.14)	4.89 (0.29)	1.48 (0.44)
45.0	2.78 (0.29)	7.36 (0.43)	3.72 (0.47)	5.35 (0.71)

^a $I = 1.0$ M (NaOH/NaBr). Rate parameters are defined in eq 5. Standard deviations are shown in parentheses.

$[(\text{tmpa})\text{Cr}(\text{O})_2\text{Cr}(\text{tmpa})]^{2+}$. Observed pseudo-first-order rate constants for fast and slow components at six temperatures in the range 20.6–45.0 °C are displayed in Table III. Plots of k_{fast} and k_{slow} vs $[\text{OH}^-]$ (Figure 4) indicate that the species responsible for fast and slow 368-nm absorbance changes both decay via two parallel pathways, zero and first order in hydroxide ion (eq 3 and 4). Rate parameters derived from linear least-squares analyses

$$k_{\text{fast}} = k_{\text{O}} + k_{\text{OH}}[\text{OH}^-] \quad (3)$$

$$k_{\text{slow}} = k_{\text{O}}^{\text{s}} + k_{\text{OH}}^{\text{s}}[\text{OH}^-] \quad (4)$$

of k_{slow} and k_{fast} vs $[\text{OH}^-]$ correlations are summarized in Table IV, and ΔH^{\ddagger} and ΔS^{\ddagger} values corresponding to the rate constants

(15) In view of the $\text{p}K_{\text{a}2}$ value of 12.4 at 25 °C and $I = 0.1$ M, the possibility that an appreciable concentration of the oxo hydroxo dimer remains in solution along with the dioxo dimer reactant in base hydrolysis kinetic studies at $[\text{OH}^-] = 0.1\text{--}1.0$ M must be considered. On this basis, the relationship between k_{obsd} and the observed rate constant corrected for the presence of unreactive oxo hydroxo dimer ($k_{\text{obsd}}^{\text{cor}}$) is $k_{\text{obsd}}^{\text{cor}} = k_{\text{obsd}}([\text{H}^+] + K_{\text{a}2})/K_{\text{a}2}$. Kinetic runs at $I = 1.0$ M showed that both the initial 368-nm absorbance and ΔA_{368} are independent of $[\text{OH}^-]$ in the interval considered, however, indicating that essentially full conversion to the dioxo dimer was achieved in the higher ionic strength kinetic medium ($K_{\text{a}2} \gg [\text{H}^+]$). For this reason, it was concluded that no correction of the observed rate constants is actually necessary.

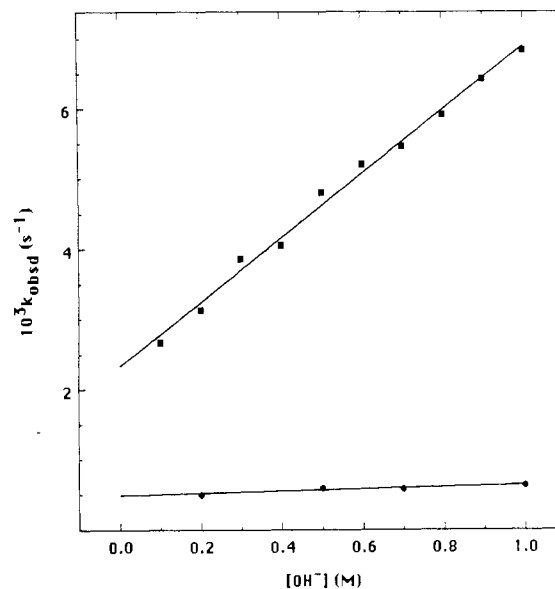


Figure 4. Plots of k_{fast} (■) and k_{slow} (●) vs $[\text{OH}^-]$ indicating the presence of both zero- and first-order terms in $[\text{OH}^-]$ for the hydrolysis of $[(\text{tmpa})\text{Cr}(\text{O})_2\text{Cr}(\text{tmpa})]^{2+}$ (fast phase) and intermediate VII (slow phase) (40.0 °C, $I = 1.0$ M (NaOH/NaBr)).

k_{O} , k_{OH} , k_{O}^{s} , and k_{OH}^{s} (from linear Eyring plots of $\ln(k/T)$ vs $1/T$) are given in Table V. Unfortunately, kinetic data for the considerably slower⁵ bpy and phen diol base hydrolysis reactions are not available for comparison with the present results.

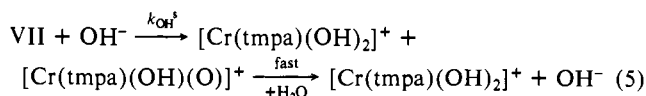
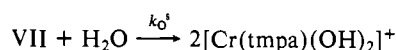
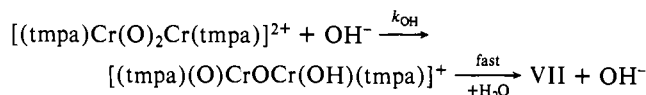
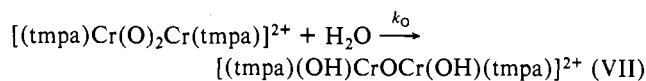
Since biphasic kinetics may reflect either consecutive or parallel first-order reaction sequences,¹⁰ the isolation and characterization of an intermediate derived from the partial base hydrolysis of $[(\text{tmpa})\text{Cr}(\text{O})_2\text{Cr}(\text{tmpa})]^{2+}$ would greatly strengthen our interpretation of the rate data. Such an intermediate was, in fact, identified through chromatographic separations (5 °C) of base hydrolysis reaction mixtures quenched before full conversion of chromium to $[\text{Cr}(\text{tmpa})(\text{OH})_2]^+$ was achieved. A solution containing 0.0594 g of I (0.05 mmol) dissolved in 24 mL of water was thermostated at 40.0 °C and mixed with 0.625 mL of 4.00 M NaOH. This reaction mixture was diluted to 25 mL and then partially quenched after 5 min by pouring into 25 mL of distilled-water ice. Upon adsorption of the mixture onto a 20×2.5 cm cation-exchange column equilibrated with 0.05 M NaOH, a leading blue band emerged and was separated cleanly from a dark green trailing fraction by elution with 0.05 M NaOH. When the eluent was changed to 0.20 M NaBr–0.05 M NaOH, the remaining chromium-containing species separated sharply into a leading deep green band, followed by a lighter green component. The 300–700-nm electronic spectra of all three bands were acquired immediately following elution, and Cr analyses were carried out so that extinction coefficients could be determined. The first and third fractions were identified as $[\text{Cr}(\text{tmpa})(\text{OH})_2]^+$ and residual reactant (as $[(\text{tmpa})\text{Cr}(\text{O})(\text{OH})\text{Cr}(\text{tmpa})]^{3+}$), respectively. The middle, deep green component (VII), which exhibited peaks at 580 nm (ϵ 85 M⁻¹ cm⁻¹) and 364 (415), may be classified as an intermediate since irreversible decay to the ultimate product, $[\text{Cr}(\text{tmpa})(\text{OH})_2]^+$, was observed when VII was allowed to stand in 0.05 M NaOH at room temperature. The intermediacy of VII is further demonstrated by the observation that the percentage of ΔA_{368} corresponding to the fast phase in kinetic studies (89%) is independent of $[\text{OH}^-]$ and agrees well with that predicted (90%) from the extinction coefficients of $[(\text{tmpa})\text{Cr}(\text{O})_2\text{Cr}(\text{tmpa})]^{2+}$ and VII at 368 nm. Species VII evidently is dimeric, since acidification of the dark green fraction (to pH 1) immediately following elution gave $[(\text{tmpa})\text{Cr}(\text{OH})_2\text{Cr}(\text{tmpa})]^{4+}$, identified from its electronic spectrum and that of ionization product III (measured after neutralizing the acidified solution with NaOH and adjusting the pH to 10). As was noted above, the tmpa diol is not regenerated by the acidification of final product V.

In separations of $[(\text{tmpa})\text{Cr}(\text{O})_2\text{Cr}(\text{tmpa})]^{2+}$ hydrolysis products carried out at pH 10.0 and 11.0, three well-separated

components were isolated as before, and fractions 1 and 3 once again contained V and III, respectively. The middle fraction attributed to the reaction intermediate was deep blue instead of dark green, however, and exhibited absorption maxima (pH 10) at 574 nm ($90 \text{ M}^{-1} \text{ cm}^{-1}$) and 372 (180). Addition of NaOH to this middle blue component (VIII) caused a reversible (with dilute HClO_4) color change to green above pH 12. This green species, an apparent ionization product of VIII, was shown to be identical with intermediate VII on the basis of its UV-visible spectrum. Attempts to isolate solids from the chromatographic fractions containing VII and VIII were futile, resulting only in quantitative conversions to monomer V.

Knowing k_{fast} and k_{slow} for the hydrolysis of $[(\text{tmpa})\text{Cr}(\text{O})_2\text{Cr}(\text{tmpa})]^{2+}$ in 0.1 M NaOH at 40.0 °C, it is possible to estimate the time at which the intermediate concentration is maximal (5 min) from the relationship $t_{\text{max}} = \ln(k_{\text{fast}}/k_{\text{slow}})/(k_{\text{fast}} - k_{\text{slow}})$.¹⁰ An attempt was made to quantitate the actual amounts of V, VII, and unreacted dioxo dimer present at t_{max} , for comparison with the theoretical values calculated from k_{fast} and k_{slow} under the reaction conditions. A solution of I (0.0397 g, 33.4 μmol) in 24 mL of H_2O was rapidly mixed with 0.625 mL of 4.00 M NaOH, and the mixture was diluted to 25 mL in a volumetric flask thermostated at 40.0 °C. After 5 min, the reaction mixture was poured into 25 mL of ice and immediately adsorbed onto a $20 \times 2.5 \text{ cm}$ cation-exchange column equilibrated with 0.05 M NaOH. Upon elution of the column with 0.05 M NaOH and 0.05 M NaOH/0.2 M NaBr, the three bands were collected as described above and quantitatively diluted in preparation for chromium analyses. Observed and calculated yields (in micromoles of Cr) of $[\text{Cr}(\text{tmpa})(\text{OH})_2]^+$ (obsd, 22.4; calcd, 5.2), intermediate VII (obsd, 31.0; calcd, 35.7), and $[(\text{tmpa})\text{Cr}(\text{O})(\text{OH})\text{Cr}(\text{tmpa})]^{3+}$ (obsd, 13.1; calcd, 25.8) are in fair agreement, with actual yields deviating as would be expected for incomplete quenching of the hydrolysis reaction after 5 min. Nevertheless, the relatively close correspondence between actual and theoretical yields of VII is a good indication that this complex is an authentic hydrolysis intermediate. Total recovery of Cr from the cation-exchange column was 99.6% (66.5 μmol).

Although the conjugate base hydrolysis mechanism (D_{cb}) is well-established for Co(III) complexes with ionizable amine ligands, Cr(III) species in general are considerably less sensitive to base hydrolysis¹⁶ and may opt for direct nucleophilic displacement of the leaving group by hydroxide ion in pathways characterized by a first-order OH^- dependence. We propose that the k_{O} and k_{OH} terms in the fast phase of $[(\text{tmpa})\text{Cr}(\text{O})_2\text{Cr}(\text{tmpa})]^{2+}$ decomposition correspond to H_2O - and OH^- -assisted bridge opening to give the intermediate VII, thought to be $[(\text{tmpa})(\text{OH})\text{CrO}(\text{OH})\text{Cr}(\text{tmpa})]^{2+}$, which then decays to $\text{Cr}(\text{tmpa})(\text{OH})_2^+$ through analogous H_2O - or OH^- -assisted oxo-bridge-cleavage steps (eq 5). The elution behavior of VII, which separates cleanly from



leading 1+ (V) and trailing 3+ (III) components on SP-Sephadex C-25 resin, is consistent with the postulated 2+ charge, and the rapid regeneration of the tmpa diol observed upon acidification of VII confirms that the hydrolysis intermediate is binuclear. Although the blue protonation product of VII observed in pH 10

Table V. Activation Parameters for the Biphasic Base Decomposition Reaction of the $[(\text{tmpa})\text{Cr}(\text{O})_2\text{Cr}(\text{tmpa})]^{2+}$ Ion^a

rate const	$k(25 \text{ }^\circ\text{C})$	ΔH^\ddagger , kcal mol ⁻¹	ΔS^\ddagger , eu
k_{O}^{\dagger}	4.7×10^{-5b}	23 (4)	-1 (11)
k_{OH}^{\dagger}	2.7×10^{-5c}	28 (3)	+14 (10)
k_{O}	3.0×10^{-4b}	19.9 (2.2)	-8 (7)
k_{OH}	5.8×10^{-4c}	22.5 (0.8)	+2 (3)

^a $I = 1.0 \text{ M}$ (NaOH/NaBr). Standard deviations are shown in parentheses. See text for rate constant definitions. ^b In s^{-1} . ^c In $\text{M}^{-1} \text{s}^{-1}$.

and 11 chromatographic separations did not survive long enough to permit a full characterization, the similarity of lowest energy d-d band positions in V (17 300 cm^{-1}) and VIII (17 400 cm^{-1}) suggests that the latter is $[(\text{tmpa})(\text{OH})\text{Cr}(\text{OH})\text{Cr}(\text{OH})(\text{tmpa})]^{3+}$.

Although the rate expression $k_{\text{obsd}} = k_{\text{O}} + k_{\text{OH}}[\text{OH}^-]$ is common for base hydrolysis reactions of mononuclear Co and Cr complexes with ionizable amine ligands,¹⁶ the finding of this rate law for both fast and slow phases of the $[(\text{tmpa})\text{Cr}(\text{O})_2\text{Cr}(\text{tmpa})]^{2+}$ alkaline decay reaction does not necessarily imply a corresponding mechanistic similarity, especially considering the absence of ionizable amine protons in the dioxo dimer. Indeed, k_{OH} and k_{OH}^{\dagger} values extrapolated to 25 °C (Table V) are 2-4 orders of magnitude smaller than the majority of room-temperature Cr(III) complex k_{OH} terms,¹⁶⁻²⁷ for which more favorable activation entropies on the order of +15-30 eu have been reported.^{17,18,23} For example, Cr-O bond breaking leading to $[(\text{NH}_3)_5\text{CrOH}]^{2+}$ in the base hydrolysis reaction of $[(\text{NH}_3)_5\text{CrONO}_2]^{2+}$ at 25 °C is characterized by k_{O} and k_{OH} values of $2.5 \times 10^{-3} \text{ s}^{-1}$ and $1.1 \times 10^{-2} \text{ M}^{-1} \text{ s}^{-1}$ ($\Delta H^\ddagger = 25.2 \text{ kcal mol}^{-1}$, $\Delta S^\ddagger = +17.0 \text{ eu}$), respectively.¹⁹ With the possible exception of the k_{OH}^{\dagger} term, ΔG^\ddagger values for both OH^- -dependent and -independent pathways in the decomposition reactions of $[(\text{tmpa})\text{Cr}(\text{O})_2\text{Cr}(\text{tmpa})]^{2+}$ and VII are governed predominantly by ΔH^\ddagger . Also notable are the relatively minor roles played by the OH^- -dependent terms in the base hydrolyses of both the dioxo tmpa dimer and VII, as measured by the ratios $k_{\text{OH}}/k_{\text{O}}$ (1.9) and $k_{\text{OH}}^{\dagger}/k_{\text{O}}^{\dagger}$ (0.6). By comparison, $k_{\text{OH}}/k_{\text{O}}$ values for $[(\text{NH}_3)_5\text{CrX}]^{2+}$ complexes are much larger and are highly sensitive to the leaving group; $\text{X} = \text{NO}_3^-$ (15) < Cl^- (196) < Br^- (690) < I^- (6900), extrapolated to zero ionic strength.¹⁶

Rate parameters reported here for the transformation of the tmpa dioxo dimer to $[(\text{tmpa})\text{Cr}(\text{OH})\text{CrO}(\text{OH})(\text{tmpa})]^{2+}$ (k_{O} path) are strikingly similar to those for the ring-opening reactions³ of $[(\text{en})_2\text{Cr}(\text{OH})_2\text{Cr}(\text{en})_2]^{4+}$ and $[(\text{NH}_3)_4\text{Cr}(\text{OH})_2\text{Cr}(\text{NH}_3)_4]^{4+}$ in acidic solution, giving the aqua hydroxo monools $[(\text{en})_2(\text{OH})\text{Cr}(\text{OH})\text{Cr}(\text{H}_2\text{O})(\text{en})_2]^{4+}$ and $[(\text{NH}_3)_4(\text{OH})\text{Cr}(\text{OH})\text{Cr}(\text{H}_2\text{O})(\text{NH}_3)_4]^{4+}$, respectively. Thus, the latter reaction^{3c} proceeds with a rate constant $k_1(25 \text{ }^\circ\text{C})$ of $1.21 \times 10^{-4} \text{ s}^{-1}$ ($\Delta H^\ddagger = 20.7 \text{ kcal mol}^{-1}$, $\Delta S^\ddagger = -7 \text{ eu}$) but is reversible ($k_{-1} = 3.80 \times 10^{-4} \text{ s}^{-1}$), unlike tmpa dioxo dimer cleavage in basic solution. Similar rate constants and activation parameters pertain to the analogous reactions of meso^{3a} and racemic^{3b} $[(\text{en})_2\text{Cr}(\text{OH})_2\text{Cr}(\text{en})_2]^{4+}$. The thermodynamic driving force in these diol to aqua hydroxo monool conversions is thought to be strongly influenced by hydrogen bonding between OH^- and H_2O ligands in the bent (Cr-O-Cr) products.³ Although the formula of intermediate VII is not known with certainty, hydrogen bonding between hydroxo substituents of a similarly bent, oxo-bridged complex $[(\text{tmpa})(\text{OH})\text{CrO}(\text{OH})(\text{tmpa})]^{2+}$ could provide part of the thermodynamic mo-

(16) Tobe, M. L. *Adv. Inorg. Bioinorg. Mech.* **1983**, 2, 1.

(17) Parris, M.; Wallace, W. J. *Can. J. Chem.* **1969**, 47, 2257.

(18) Guastalla, G.; Swaddle, T. W. *Can. J. Chem.* **1974**, 52, 527.

(19) Campi, E.; Ferguson, J.; Tobe, M. L. *Inorg. Chem.* **1970**, 9, 1781.

(20) Lichtig, J.; Tobe, M. L. *Inorg. Chem.* **1978**, 17, 2442.

(21) Levine, M. A.; Jones, T. P.; Harris, W. E.; Wallace, W. J. *J. Am. Chem. Soc.* **1961**, 83, 2453.

(22) Pearson, R. G.; Munson, R. A.; Basolo, F. *J. Am. Chem. Soc.* **1958**, 80, 504.

(23) Yang, D.; House, D. A. *Inorg. Chem.* **1982**, 21, 2999.

(24) Dawson, B. S.; House, D. A. *Inorg. Chem.* **1977**, 16, 1354.

(25) House, D. A. *Coord. Chem. Rev.* **1977**, 23, 223.

(26) House, D. A. *Inorg. Chem.* **1988**, 27, 2587.

(27) Olsen, D. C.; Garner, C. S. *Inorg. Chem.* **1963**, 2, 558.

tivation for decomposition of the dioxo dimer and the enhanced kinetic stability of the intermediate relative to that of the doubly bridged reactant. In any case, the vast difference between the UV-vis spectra of VII and the well-characterized $[(\text{tmpa})\text{Cr}(\text{SCN})\text{Cr}(\text{NCS})(\text{tmpa})]^{2+}$ ion⁴ rules out the classification of the base hydrolysis intermediate as a linear, μ -oxo dimer. Mechanistic studies of the base hydrolysis reactions of $[(\text{tmpa})(\text{SCN})\text{Cr}(\text{O})\text{Cr}(\text{NCS})(\text{tmpa})]^{2+}$ and related dimers are currently in progress.¹⁴

Acknowledgment is made to the donors of the Petroleum Research Fund, administered by the American Chemical Society, for support of this research. We also thank the Robert A. Welch Foundation (Grant D-735) for partial financial support of this

project and Dr. Charles F. Campana of Nicolet Instrument Corp. for performing the X-ray crystallographic measurements on $[(\text{tmpa})\text{Cr}(\text{OH})_2\text{Cr}(\text{tmpa})]\text{Br}_4 \cdot 8\text{H}_2\text{O}$.

Registry No. I, 117603-54-0; II, 117773-50-9; III, 117709-84-9; IV, 117689-06-2; $[\text{H}_3\text{tmpa}](\text{ClO}_4)_3$, 117689-07-3; $[(\text{bpy})_2\text{Cr}(\text{OH})_2\text{Cr}(\text{bpy})_2](\text{ClO}_4)_4 \cdot 2\text{H}_2\text{O}$, 31418-78-7; $[(\text{phen})_2\text{Cr}(\text{OH})_2\text{Cr}(\text{phen})_2](\text{ClO}_4)_4 \cdot 3\text{H}_2\text{O}$, 31282-13-0; $[(\text{tmpa})\text{Cr}(\text{O})_2\text{Cr}(\text{tmpa})]^{2+}$, 117689-08-4; 2-picoyl chloride hydrochloride, 6959-47-3; bis(2-pyridylmethyl)amine, 1539-42-0.

Supplementary Material Available: Structure determination summary and listings of bond lengths and angles, anisotropic displacement parameters, and H atom coordinates and isotropic displacement parameters for $[(\text{tmpa})\text{Cr}(\text{OH})_2\text{Cr}(\text{tmpa})]\text{Br}_4 \cdot 8\text{H}_2\text{O}$ (6 pages). Ordering information is given on any current masthead page.

Contribution from the Institut de chimie, Université de Neuchâtel, Avenue de Bellevaux 51, CH-2000 Neuchâtel, Switzerland

Early Stages of the Hydrolysis of Chromium(III) in Aqueous Solution. 4. Stability Constants of the Hydrolytic Dimer, Trimer, and Tetramer at 25 °C and $I = 1.0 \text{ M}^1$

Hans Stünzi,*² Leone Spiccia,³ François P. Rotzinger,⁴ and Werner Marty[†]

Received March 8, 1988

Addition of up to 0.8 equiv of base to aqueous Cr^{3+} results in the formation of Cr(III) hydrolytic oligomers in homogeneous solution. The evolution of these species was followed over a period of 4 years at 25 °C and $I = 1.0 \text{ M}$ (NaClO_4) by pH measurement, chromatographic separation, and determination of the Cr content of each oligomer fraction. After the addition of base, oligomerization caused a relatively rapid drop in monomer concentration and pH. The concentration of the dimer, $\text{Cr}_2(\text{OH})_2^{4+}$, reached its maximum after a few days, while the trimer concentration increased monotonously throughout the reaction and $\text{Cr}_3(\text{OH})_4^{5+}$ became the dominant oligomer. The concentration of the tetramer, $\text{Cr}_4(\text{OH})_6^{6+}$, was rather constant after a few months. The higher oligomers were formed within a few days and subsequently decayed, contributing to the stabilization of pH after a few weeks. From the composition and the pH of Cr(III) solutions kept at 25 °C for 4 years, the cumulative stability constants $\beta_{ap} = [\text{Cr}_q(\text{OH})_p^{(3q-p)+}][\text{H}^+]^p/[\text{Cr}^{3+}]^q$ have been determined: For the fully protonated oligomers the values are $\log \beta_{22} = -5.25 \pm 0.04$, $\log \beta_{34} = -8.72 \pm 0.06$, and $\log \beta_{46} = -13.86 \pm 0.15$, and for the deprotonated species the values are $\log \beta_{23} = -8.93$, $\log \beta_{35} = -13.07$, and $\log \beta_{47} = -16.41$. Combination with the pK_a values of Cr^{3+} and the oligomers gives the stepwise stability constants for the addition of $\text{Cr}(\text{OH})_2^+$ to Cr^{3+} and $\text{Cr}[\text{Cr}(\text{OH})_2]_{q-1}^+$: $\log K_{22} = 5.1$, $\log K_{34} = 6.9$, $\log K_{46} = 5.2$, and $\log K_{58} < 6.4$. For the addition of $\text{Cr}(\text{OH})_2^+$ to either $\text{Cr}(\text{OH})_2^{2+}$ or the monodeprotonated oligomers, one obtains $\log K_{23} = 5.8$, $\log K_{35} = 6.3$, $\log K_{47} = 7.0$, and $\log K_{59} < 6.0$.

Introduction

The determination of the stability of individual oligomeric intermediates, formed as a result of hydrolytic polymerization, is a classical theme in the coordination chemistry of metal ions in aqueous solution. Under the impact of Sillén and his group,⁵ potentiometric titration methods have been used extensively to study the hydrolysis of metal ions.⁶ Thus, potentiometric data are subjected to mathematical fitting procedures to determine the predominant solution species as well as their respective stability constants. In this process, the acid dissociation constants for each oligomer must also be taken into account. Due to the complicated nature of these systems, differences of opinion concerning the dominant oligomers for a particular metal ion are not uncommon.⁷ Nevertheless, a considerable body of valuable and reliable information covering a variety of metal centers is available.⁶ Of relevance to the work discussed here are recent pH-metric studies on the hydrolytic polymerization of Cr(III).⁸⁻¹⁰

For kinetically inert metal centers, protonation/deprotonation reactions are rapid while substitution processes, involved in the formation of oligomers, are slow. Thus, alkalization deprotonates the aqua ions and promotes polymerization through the resulting conjugate bases, which are much more reactive in substitution processes than fully protonated aqua ions and oligomers.¹ Reacidification protonates the oligomers, thereby preventing further polymerization. At the same time, the acid cleavage of the protonated oligomers is slow,¹¹ and this inertness allows their isolation by chromatographic techniques and their further in-

Table I. Evolution of Species in Solutions of the Chromium Aqua Ion ($Z = 0.3$)^a

time, h or days	pH	monomer %	dimer %	trimer %	tetramer %	higher %	sum, ^b mM	soln ^c
0.5 ^d	3.93	98.7	0.5	0.1	0.1	0.6	39.6	D
1.0	3.92	97.2	1.4	0.2	0.1	1.1	40.2	D
2.0	3.89	95.8	2.3	0.7	0.2	1.1	39.4	A
4.0	3.78	94.5	3.1	0.6	0.2	1.6	39.3	A
6.0	3.68	91.6	3.9	0.6	0.5	3.4	39.0	B
8.0	3.57	89.4	4.5	0.7	0.3	5.2	39.3	C
12.0	3.35	86.7	4.7	1.1	0.7	6.8	40.4	E
18.0	3.10	83.4	5.2	2.1	1.2	8.2	40.2	E
1 ^e	3.09	81.8	6.3	2.9	1.1	7.8	39.0	K
1	2.96	80.8	6.1	2.6	1.2	9.3	38.9	A
2	2.84	79.1	6.4	3.5	1.5	9.6	39.3	F
3	2.84	79.1	6.5	3.6	1.9	8.8	39.0	B
4	2.84	78.9	6.4	3.6	1.8	9.3	39.6	A
6	2.84	79.3	6.4	3.2	1.9	9.2	38.9	B
10	2.88	79.3	6.5	3.3	1.7	9.2	40.1	E
20	2.85	78.2	6.4	5.7	1.6	8.3	38.7	B
32	2.87	78.6	6.4	6.2	1.8	7.1	38.8	G
64	2.82	76.3	6.4	8.4	2.3	6.5	39.4	G
122	2.80	75.7	7.1	9.8	2.7	4.8	38.5	G
155	2.76	75.7	5.9	13.0	3.2	2.2	38.4	O
213	2.76	74.6	6.1	13.7	2.6	3.0	39.1	G
262	2.74	74.1	6.1	14.5	2.5	2.7	38.9	G
406	2.69	73.1	6.0	16.5	2.1	2.3	38.6	G
1613	2.70	72.9	5.6	17.4	2.2	1.9	37.9	G
1700	2.66	74.7	5.6	15.9	2.2	1.7	40.2	O

^a $I = 1.0 \text{ M}$ (NaClO_4); 25 °C. ^b Total (eluted) chromium concentration. ^c Identifier for different solutions. ^d Hours. ^e Days.

vestigation. In the case of Cr(III), recent progress in the separation of hydrolytic oligomers¹¹ has led to the characterization of the

* To whom correspondence should be addressed.

[†] Deceased September 20, 1986.